Microscopic model of K^-NN absorption and its application in kaonic atoms calculations

Jaroslava Óbertová
Nuclear Physics Institute, Řež
& FNSPE, CTU in Prague

Àngels Ramos
University of Barcelona

Eli Friedman
Hebrew University, Jerusalem

Jiří Mareš
Nuclear Physics Institute, Řež

Joint THEIA-STRONG2020 and JAEA/Mainz REIMEI Web-Seminar
3 February, 2021

Outline

- Introduction
- Microscopic model for $K^- NN$ absorption in nuclear matter
- Kaonic atoms calculations
- Conclusions

My current project 'Ema'

Introduction

- K^- multi-nucleon absorption fraction in the surface region of atomic nuclei represents about 20%

  NC 53 (1968) 313 (Berkeley), *NPB 35 (1971) 332 (BNL)*, *NC 39A (1977) 538 (CERN)*

- K^- multi-nucleon absorption in atoms described by phenomenological optical potential

  E. Friedman, A. Gal, NPA 959 (2017) 66

- Model for K^-NN absorption in nuclear matter using free-space chiral amplitudes

  T. Sekihara et al., PRC 86 (2012) 065205

- New experimental data on K^-NN absorption (AMADEUS@DAΦNE)

  K. Piscicchia et al., PLB 782 (2018) 339

  R. Del Grande et al., EPJ C79 (2019) 190

- Solid microscopic model for K^-NN absorption needed

Free-space $K^- p$ amplitudes in various chiral models

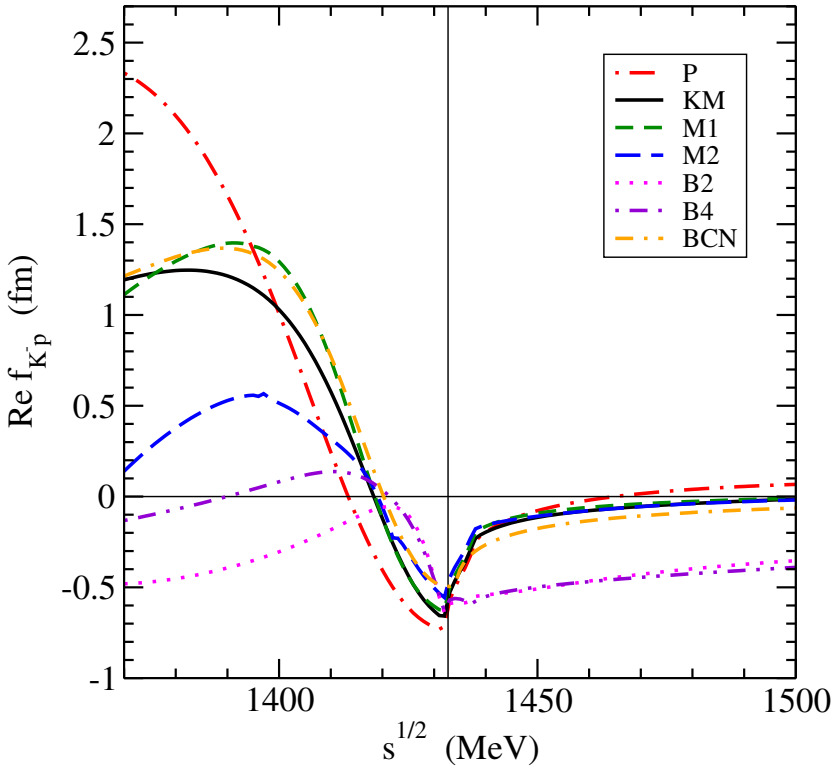

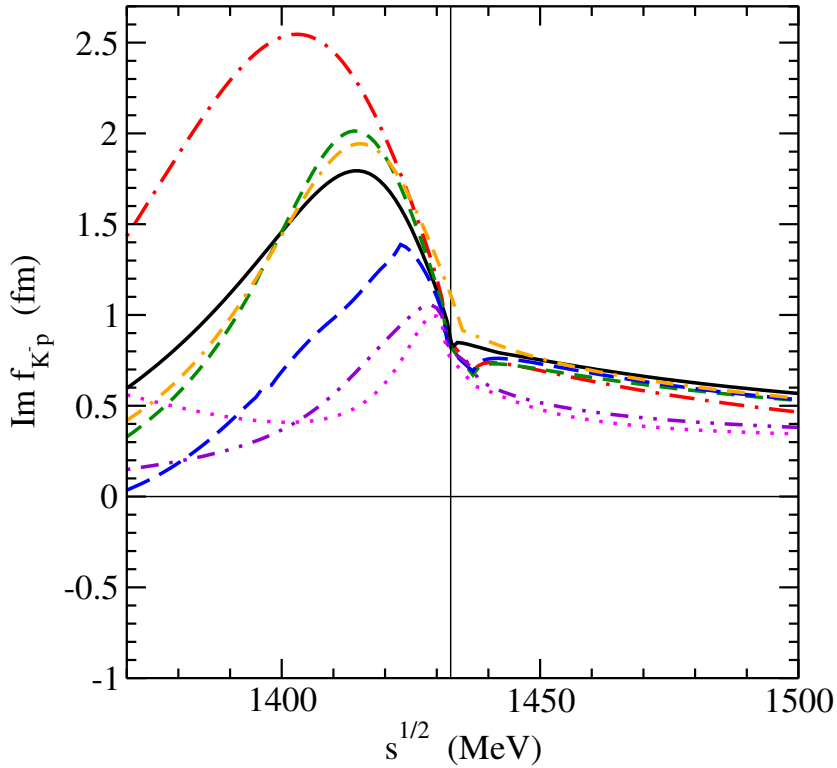

Prague (P)	*A. Cieply, J. Smejkal, Nucl. Phys. A 881 (2012) 115*
Kyoto-Munich (KM)	*Y. Ikeda, T. Hyodo, W. Weise, Nucl. Phys. A 881 (2012) 98*
Murcia (M1 and M2)	*Z. H. Guo, J. A. Oller, Phys. Rev. C 87 (2013) 035202*
Bonn (B2 and B4)	*M. Mai, U.-G. Meißner, Nucl. Phys. A 900 (2013) 51*
Barcelona (BCN)	*A. Feijoo, V. Magas, A. Ramos, Phys. Rev. C 99 (2019) 035211*

Free-space $K^- n$ amplitudes

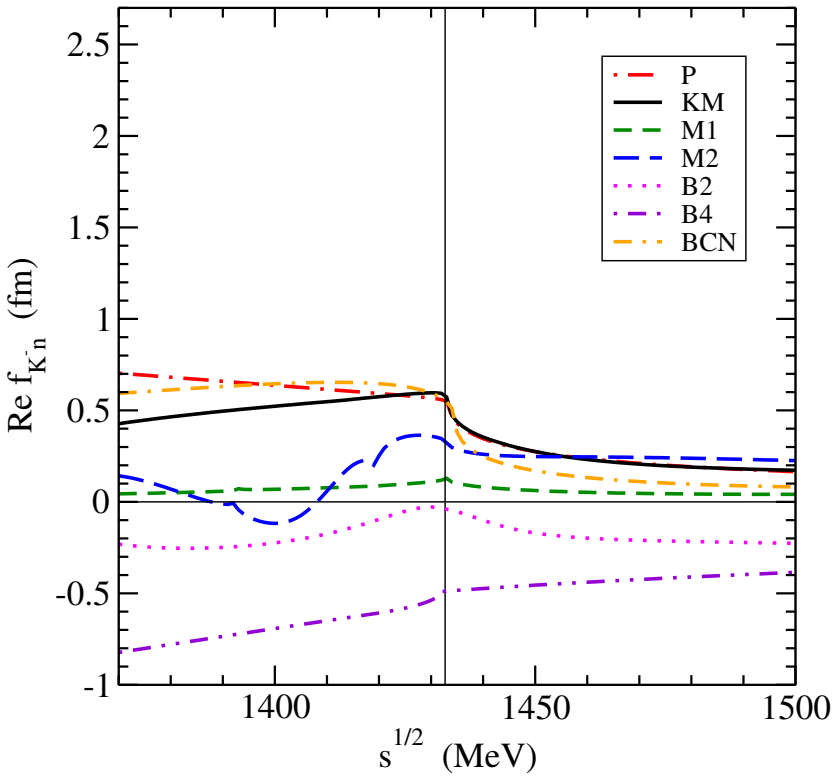

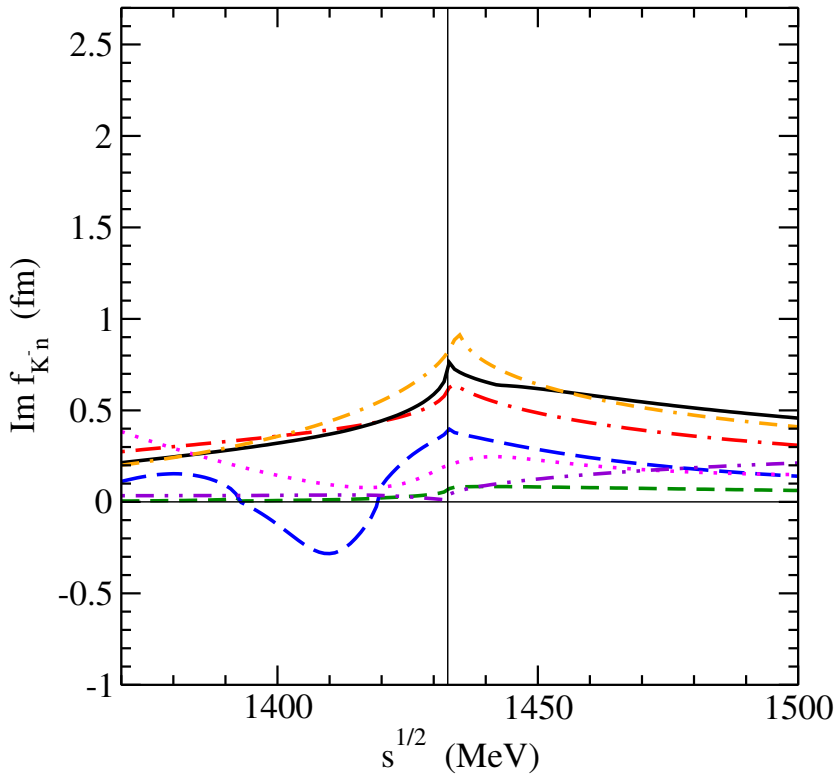

Kaonic atoms

- Info about $K^- N$ interaction below threshold provided by kaonic atoms

  65 data points (energy shifts, widths, yields=upper level widths) from CERN, Argonne, RAL, BNL

- Chirally motivated models fail to describe kaonic atom data

  E. Friedman, A. Gal, NPA 959 (2017) 66

model	B2	B4	M1	M2	P	KM
$\chi^2(65)$	1174	2358	2544	3548	2300	1806

Multinucleon processes

- Chiral models include only $K^- N \to \pi Y$ ($Y = \Lambda, \Sigma$) decay channel
- K^- interactions with two and more nucleons should be included, (e.g., $K^- + N + N \to Y + N$) $\leftarrow$ analysis of kaonic atom data

  E. Friedman, A. Gal, NPA 959 (2017) 66

$$2\mathrm{Re}(\omega_{K^-}) V_{K^-}^{(2)} = -4\pi B (\frac{\rho}{\rho_0})^{\alpha} \rho \ ,$$

where B is a complex amplitude, ρ is nuclear density distribution, ρ_0 is saturation density and α is positive

- Amplitude B fitted for each chiral model separately
- $\chi^2(65)$ goes down to 105 - 125

Single- vs. multi-nucleon processes

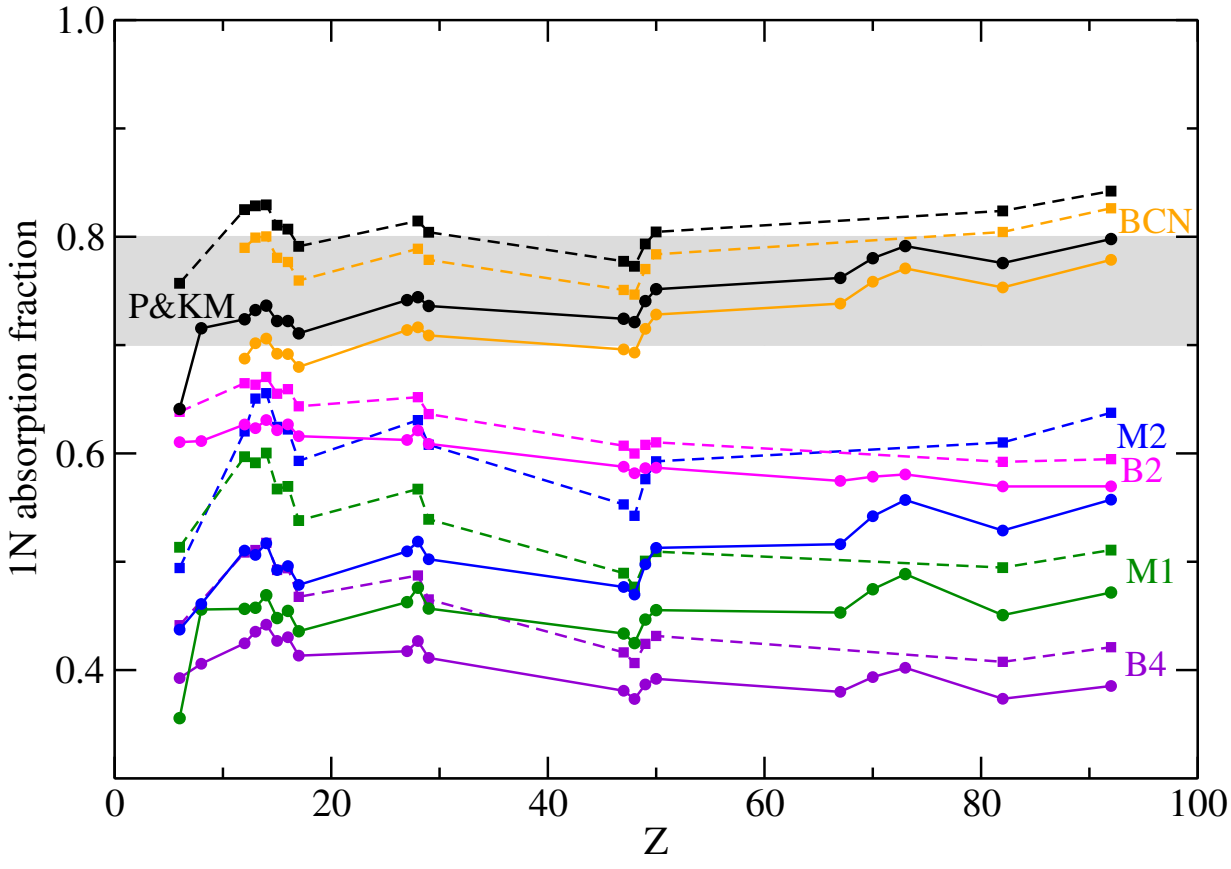

- Fraction of *single-nucleon* absorption 0.75 ± 0.05 (average value) used as an additional constraint.

$\rightarrow$ Only P, KM and BCN models found acceptable in kaonic atom analysis

E. Friedman, A. Gal, NPA 959 (2017) 66

K. Piscicchia, talk at THEIA-STRONG2020 Web-Seminar,20 December 2020

Outcome of the measurement

Investigated using: K^- "n" $^3He \rightarrow \Lambda\pi^- {}^3He$

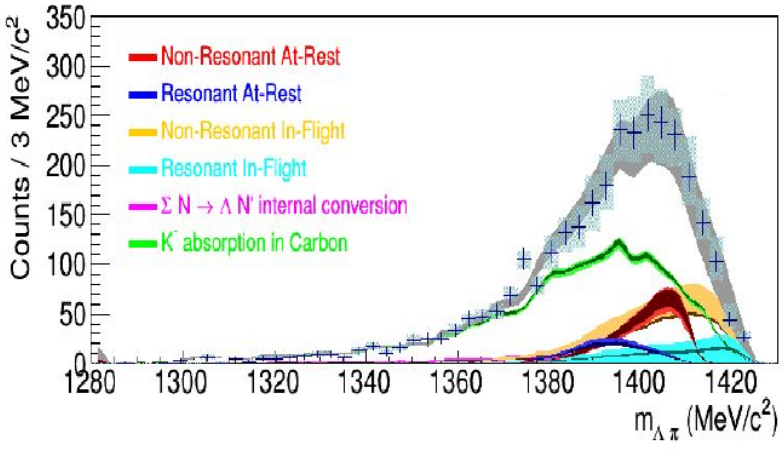

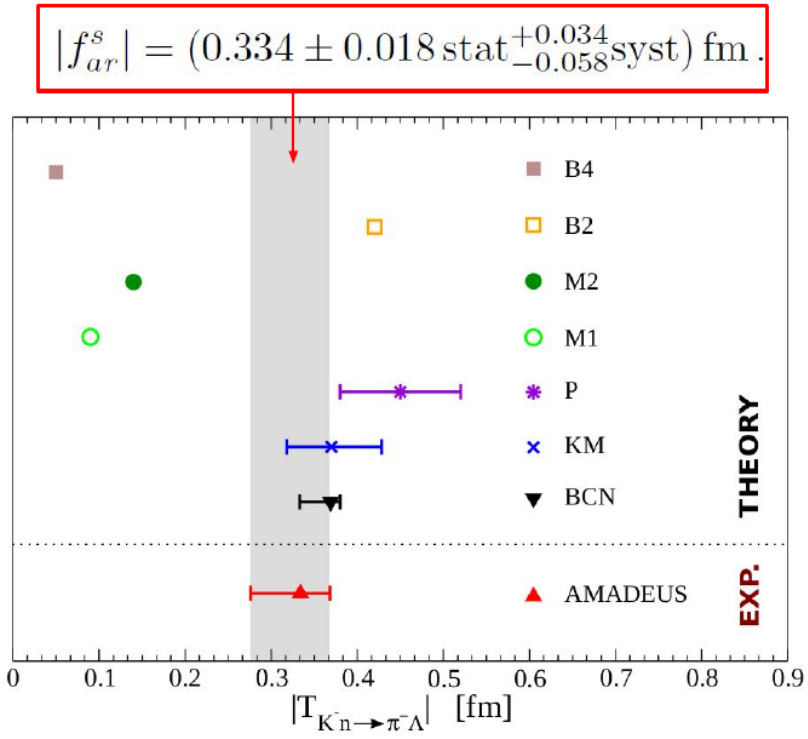

[K. Piscicchia, S. Wycech, L. Fabbietti et al. Phys.Lett. B782 (2018) 339-345]
[K. Piscicchia, S. Wycech, C. Curceanu, Nucl. Phys. A 954 (2016) 75-93]

Microscopic model for K^-NN absorption in nuclear matter

We have developed a microscopic model for K^- two-nucleon absorption in symmetric nuclear matter

J. Hrtánková, À. Ramos, PRC 101 (2020) 035204

- based on a meson-exchange approach

  H. Nagahiro et al., PLB 709 (2012) 87
- employing P and BCN chiral K^-N amplitudes
- considering Pauli correlations in the medium for K^-N amplitudes
- real part of the K^-NN optical potential evaluated as well
- K^-N optical potential derived within the same approach

K^-N absorption in nuclear matter

$$K^-N \to \pi Y \quad (Y = \Lambda, \Sigma)$$

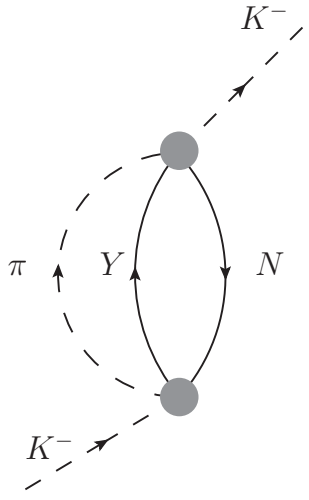

- K^-N self-energy

$$\Pi_{K^-N\to\pi Y}(\vec{p}, p_0) = \mathrm{i}\,|t_{K^-N\to\pi Y}|^2 \int \frac{d^4q}{(2\pi)^4} U_{YN}(p-q) \frac{1}{q^2 - m_\pi^2 + \mathrm{i}\eta}$$

t - two-body t-matrix; U - Lindhard function

p - kaon 4-momentum; q - meson 4-momentum

K^-NN absorption in nuclear matter

$$K^- + N + N \to Y + N \quad (Y = \Lambda, \Sigma)$$

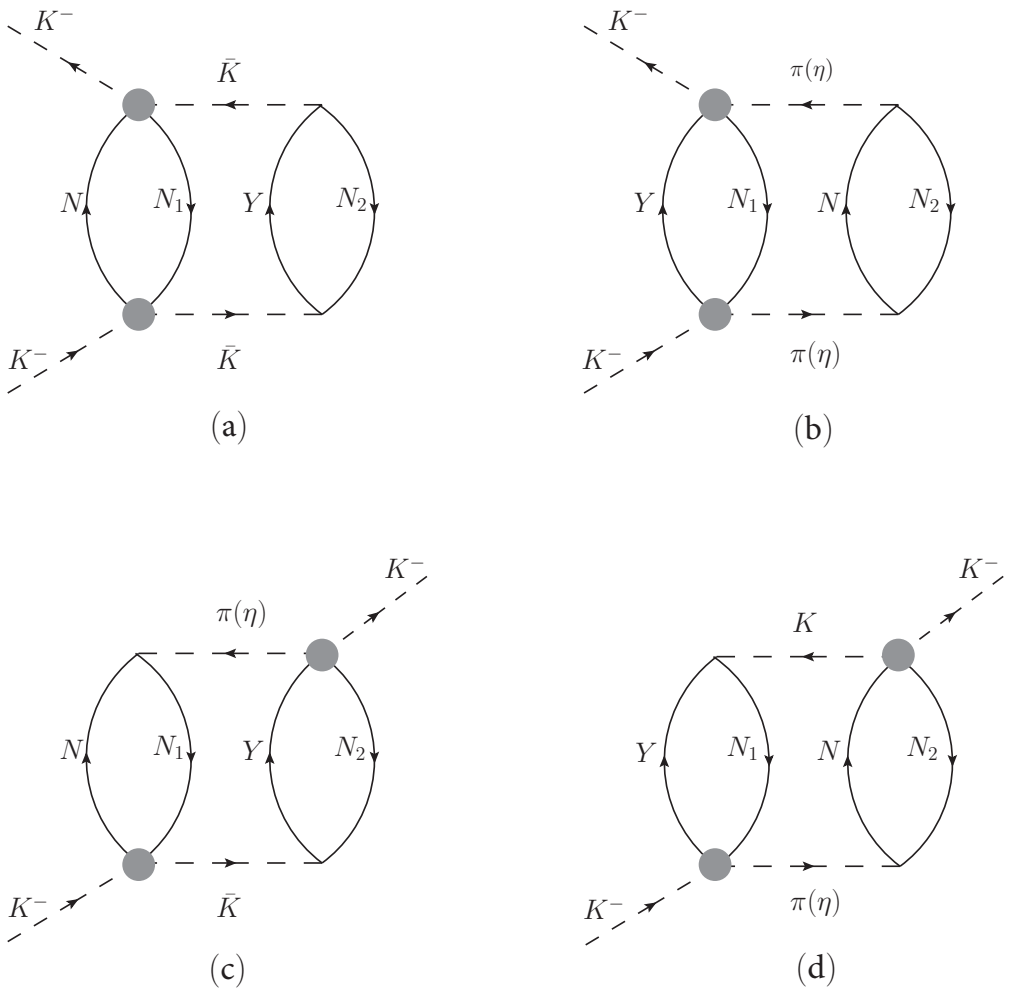

Fig.1: Two-fermion-loop (2FL) Feynman diagrams for non-mesonic K^- absorption on two nucleons N_1, N_2 in nuclear matter. The shaded circles denote the K^-N t-matrices derived from a chiral model.

K^-NN absorption in nuclear matter

- K^-NN self-energy from a direct 2FL diagram

$$\Pi^{\mathrm{2FL}}_{K^-NN}(\vec{p},p_0) = -\,\mathrm{i}\,t_{B_1 x}\,t^*_{B_1 x}\,V_{B_2 N_2 x}\,V_{B_2 N_2 x}\int \frac{d^4q}{(2\pi)^4}\,U_{B_1 N_1}(p-q)\,U_{B_2 N_2}(q)$$
$$\times\,(-\vec{q}^{\,2})\,\frac{F(\vec{q})}{q^2-m_x^2+\mathrm{i}\eta}\;\frac{F(\vec{q})}{q^2-m_x^2+\mathrm{i}\eta}\;,$$

$x = K^-, \bar{K}^0, \pi,\ \eta$; t - two-body t-matrices; $B_1, B_2 = N, Y$

V - meson-baryon-baryon couplings; U - Lindhard function

p - kaon 4-momentum, q - meson 4-momentum,

$F(\vec{q}) = \dfrac{\Lambda_C^2}{\Lambda_C^2+\vec{q}^{\,2}}$ - form factor, Λ_C - cut-off parameter

- Contributions from diagrams (c) and (d) are zero due to null trace over spins

K^-NN absorption in nuclear matter

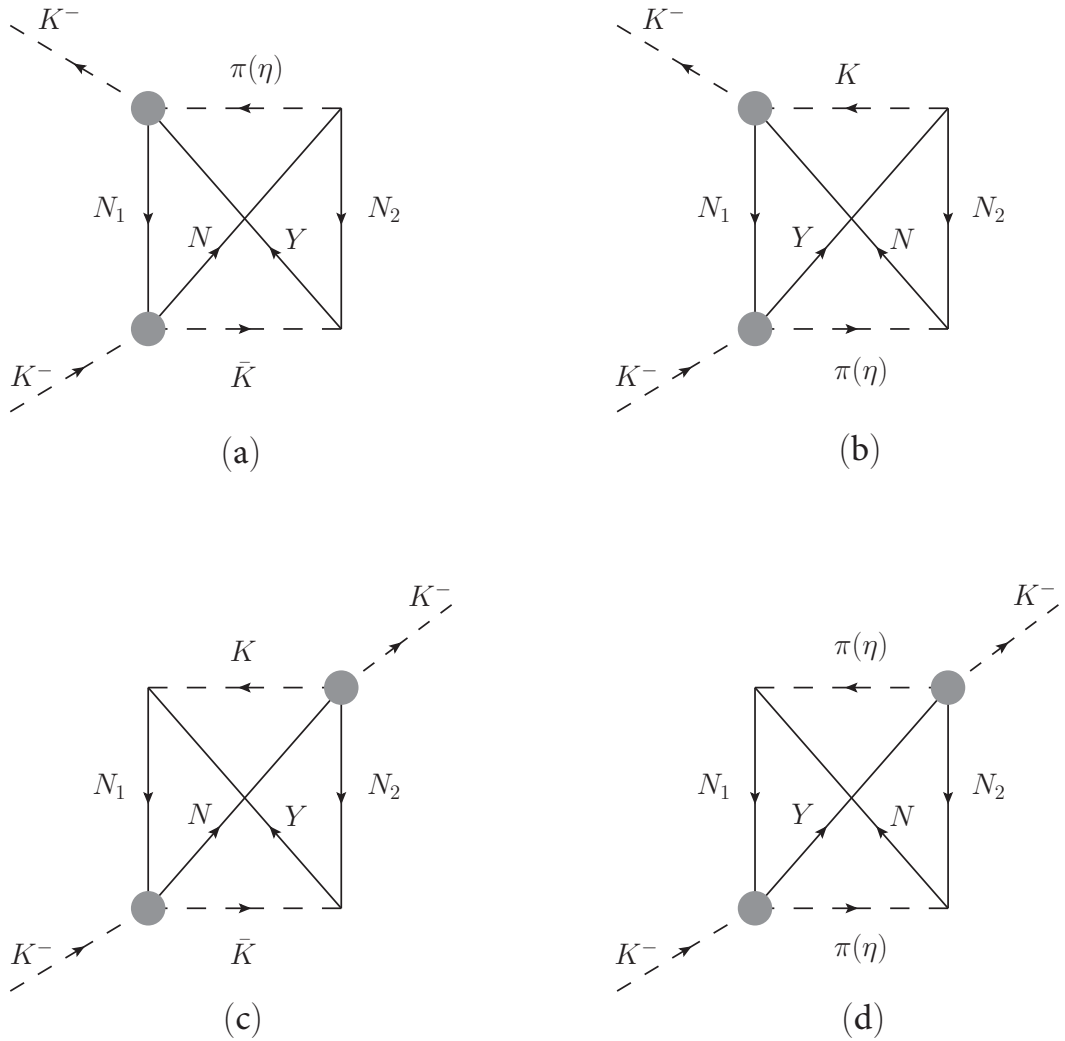

Fig.2: One-fermion-loop (1FL) Feynman diagrams for non-mesonic K^- absorption on two nucleons N_1, N_2 in nuclear matter. The shaded circles denote the K^-N t-matrices derived from a chiral model.

$K^- NN$ absorption in nuclear matter

- $K^- NN$ self-energy from an exchange 1FL diagram

$$\Pi^{1\mathrm{FLA}}_{K^-NN}(\vec{p}, p_0) = -\,\mathrm{i}\, t_{B_1 x_1}\, t^*_{B_2 x_2}\, V_{B_2 N_2 x_1}\, V_{B_1 N_2 x_2} \int \frac{d^4 q}{(2\pi)^4} (+2\vec{q}^{\,2})$$

$$\times \int \frac{d^4 j}{(2\pi)^4} G_{N_1}(j) G_{B_1}(j + p - q) \int \frac{d^4 k}{(2\pi)^4} G_{N_2}(k) G_{B_2}(q + k)$$

$$\times \frac{1}{q^2 - m^2_{x_1} + \mathrm{i}\eta} \; \frac{1}{q'^{\,2} - m^2_{x_2} + \mathrm{i}\eta} =$$

$$= \mathrm{i}\, t_{B_1 x_1}\, t^*_{B_2 x_2}\, V_{B_2 N_2 x_1}\, V_{B_1 N_2 x_2} \frac{1}{2} \int \frac{d^4 q}{(2\pi)^4} U_{B_1 N_1}(p - q) U_{B_2 N_2}(q)$$

$$\times \vec{q}^{\,2} \frac{F(\vec{q})}{q^2 - m^2_{x_1} + \mathrm{i}\eta} \; \frac{F(\vec{q'})}{q'^{\,2} - m^2_{x_2} + \mathrm{i}\eta}$$

G - baryon propagator in the medium; j, k - nucleon 4-momenta

$K^- NN$ absorption in nuclear matter

- K^- self-energy related to optical potential $V_{K^-} = \frac{\Pi_{K^-}}{2E_{K^-}}$
- $V_{K^-N} = \sum_{channels} V_{K^-N \to \pi Y}$
- $V_{K^-NN} = \sum_{\text{channels}} V^{\text{2FL}}_{K^-NN} + V^{\text{1FL}}_{K^-NN}$

  $\to$ contributions from 37 2FL and 28+33 1FL diagrams

Table 1: All considered channels for mesonic and non-mesonic K^- absorption in matter.

K^-N	$\to \pi Y$	$K^-N_1N_2$	$\to YN$
K^-p	$\to \pi^0\Lambda$	K^-pp	$\to \Lambda p$
	$\to \pi^0\Sigma^0$		$\to \Sigma^0 p$
	$\to \pi^+\Sigma^-$		$\to \Sigma^+ n$
	$\to \pi^-\Sigma^+$	$K^-pn(np)$	$\to \Lambda n$
K^-n	$\to \pi^-\Lambda$		$\to \Sigma^0 n$
	$\to \pi^-\Sigma^0$		$\to \Sigma^- p$
	$\to \pi^0\Sigma^-$	K^-nn	$\to \Sigma^- n$

$K^- N$ free-space vs. Pauli blocked scattering amplitudes

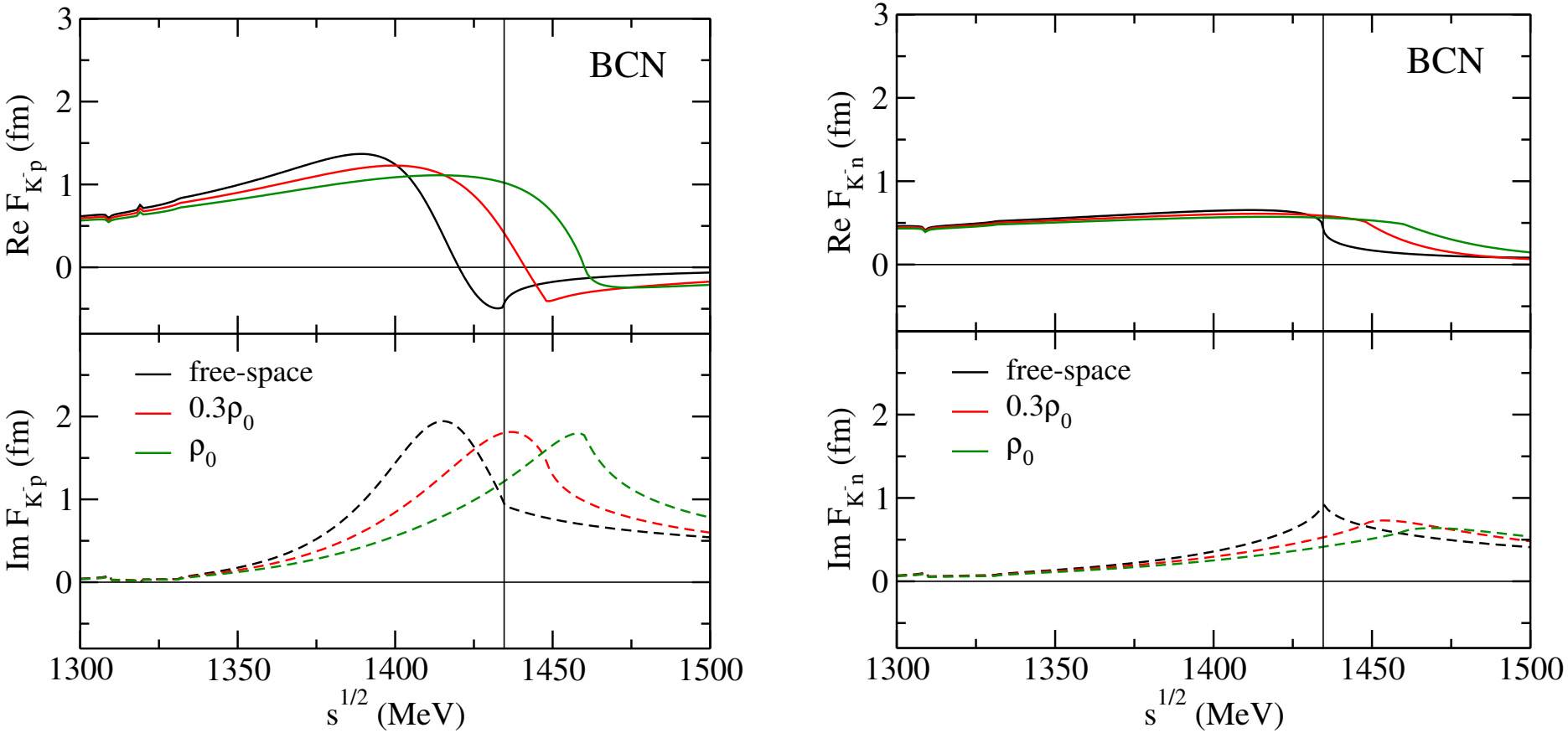

Fig.3: Comparison of $K^- p$ and $K^- n$ free-space (black) and Pauli blocked amplitudes at two different nuclear matter densities: $0.3\rho_0$ (red) and ρ_0 (green), calculated in the BCN model.

Energies probed below K^-N threshold

- Energy shift $\delta\sqrt{s} = \sqrt{s} - E_{\rm th}$ where $\sqrt{s} = \sqrt{(E_{K^-} + E_F)^2 - \frac{3}{5}k_F^2 - p_{K^-}^2 \frac{\rho}{\rho_0}}$,

$E_{\rm th} = m_N + m_{K^-}$, $E_F = \sqrt{m_N^2 + \frac{3}{5}k_F^2} + V_N \frac{\rho}{\rho_0}$ with $V_N = -50$ MeV,

k_F - Fermi momentum, $\rho_0 = 0.169$ fm^{-3}, $E_{K^-} = m_{K^-} - B_{K^-}\frac{\rho}{\rho_0}$

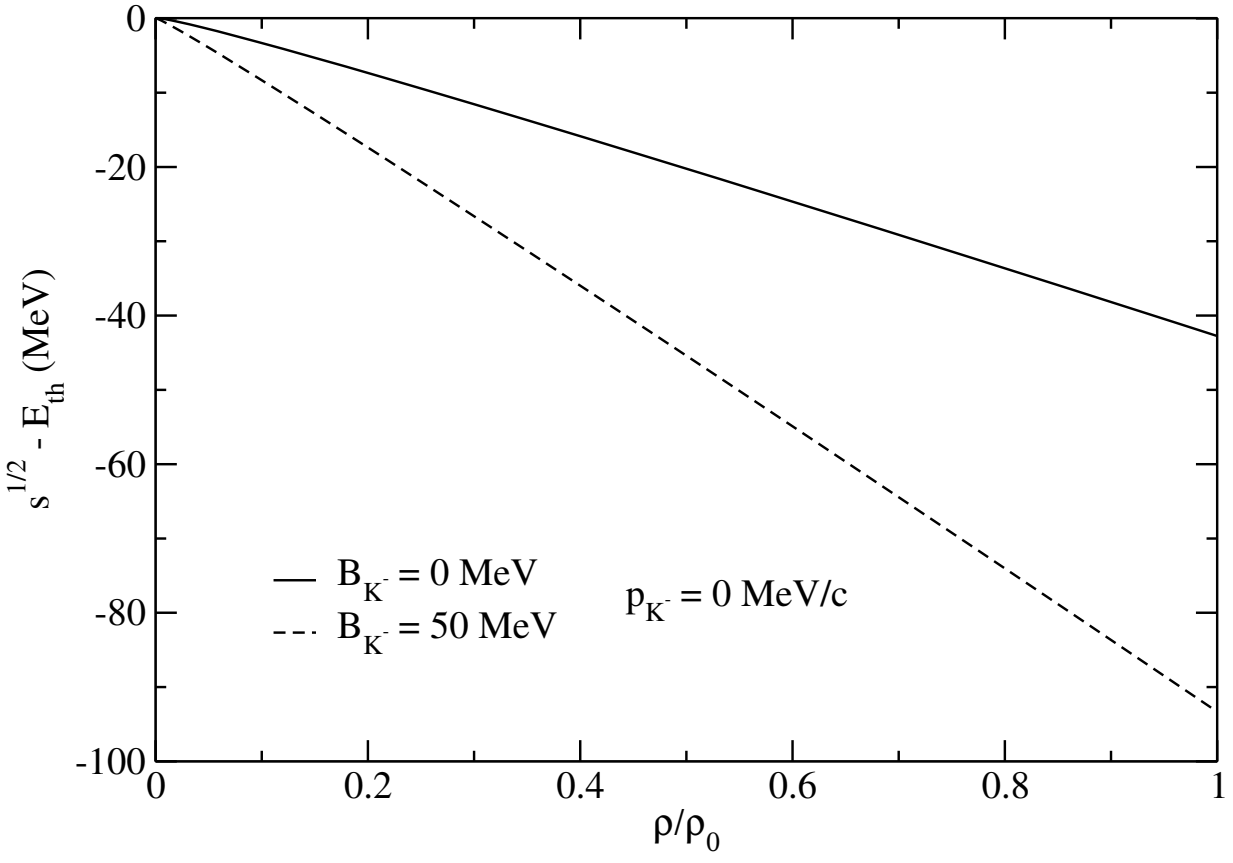

K^- potential in nuclear matter - medium effects

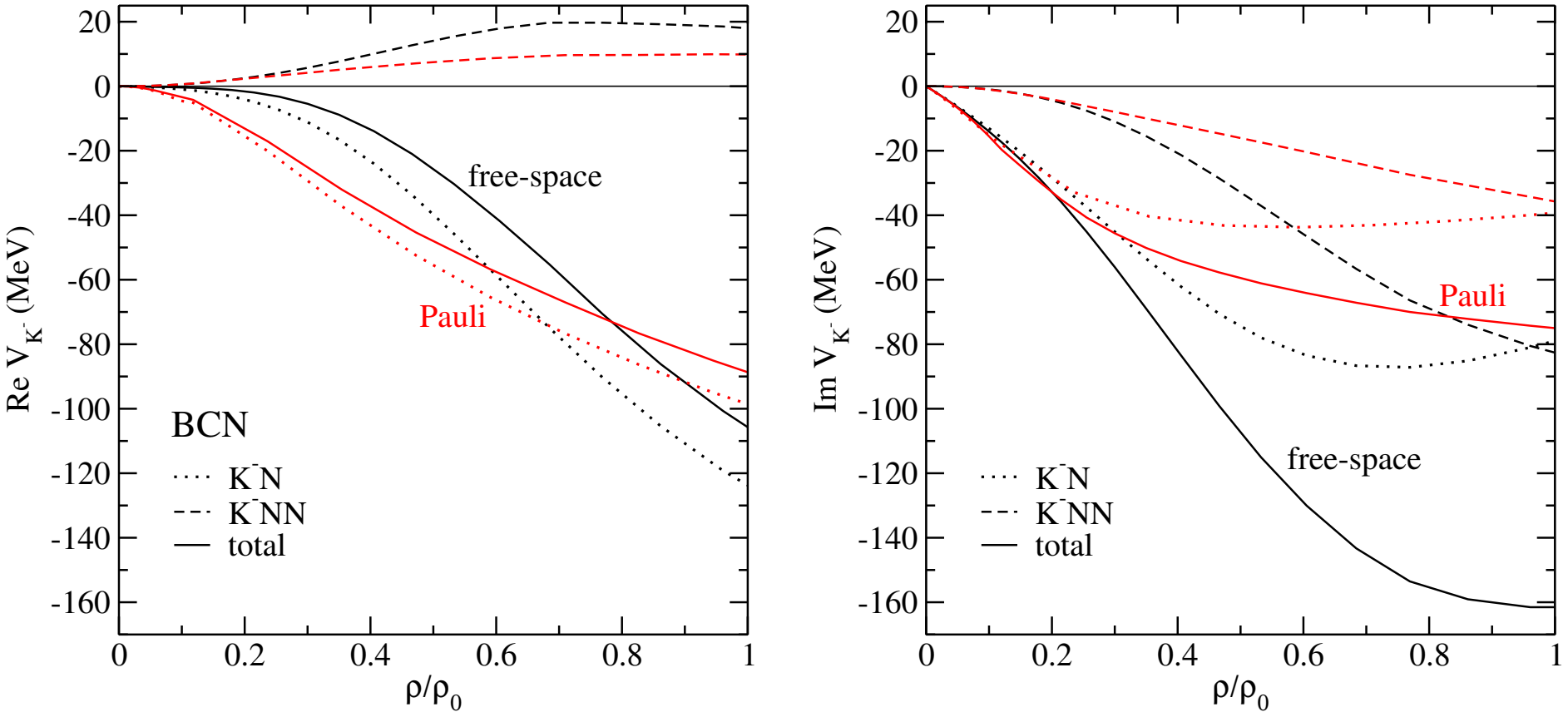

Fig.4: The real (left) and imaginary (right) parts of the K^-N, K^-NN, and total optical potentials as a function of relative density, calculated using the free-space (black) and Pauli blocked (red) BCN amplitudes for $B_{K^-} = 0$ MeV and $p_{K^-} = 0$ MeV/c.

Momentum dependence

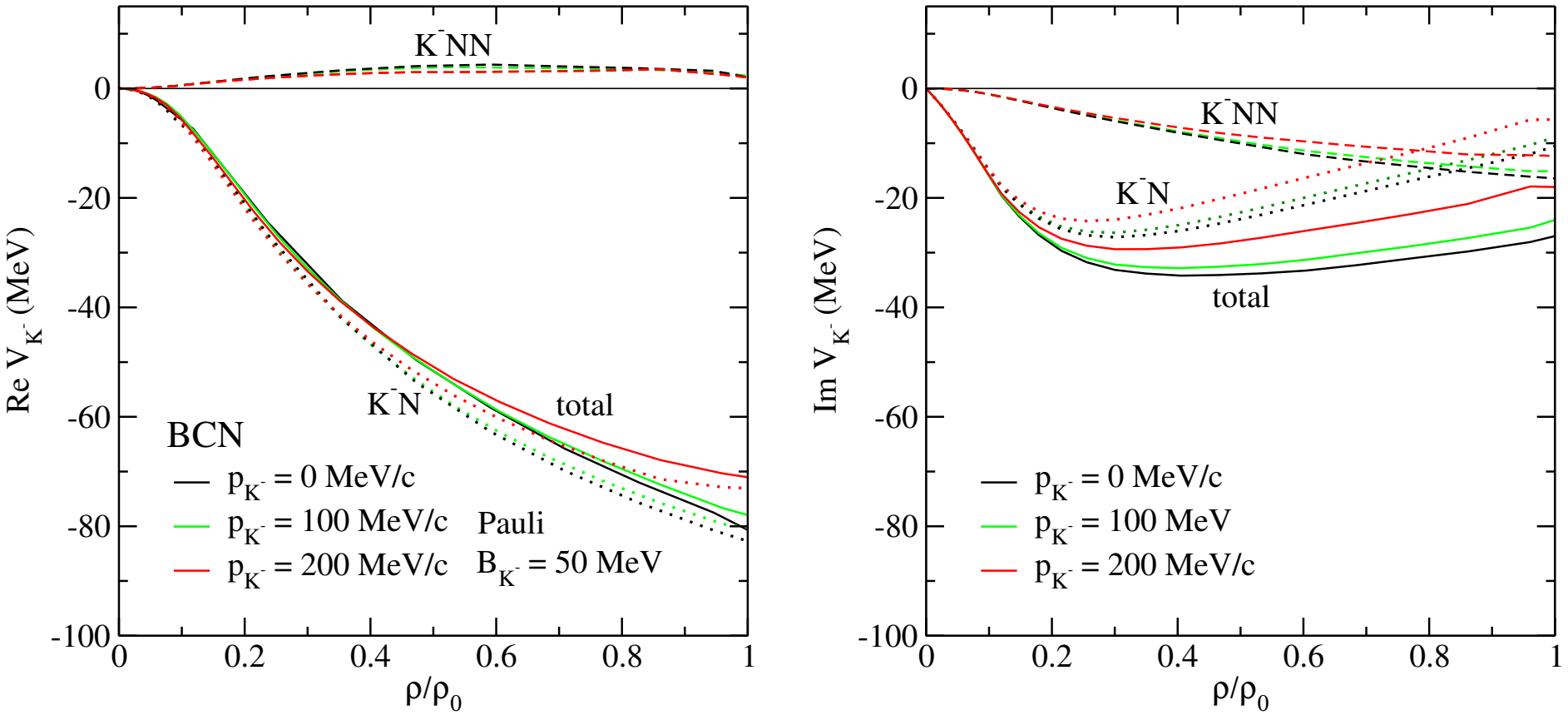

Fig.5: The real (left) and imaginary (right) parts of the K^-N (dotted), K^-NN (dashed), and total (solid) optical potentials as a function of relative density ρ/ρ_0, calculated for $B_{K^-} = 50$ MeV at ρ_0 and three different kaon momenta p_{K^-} using the Pauli blocked BCN amplitudes.

K^-N and K^-NN absorption fractions

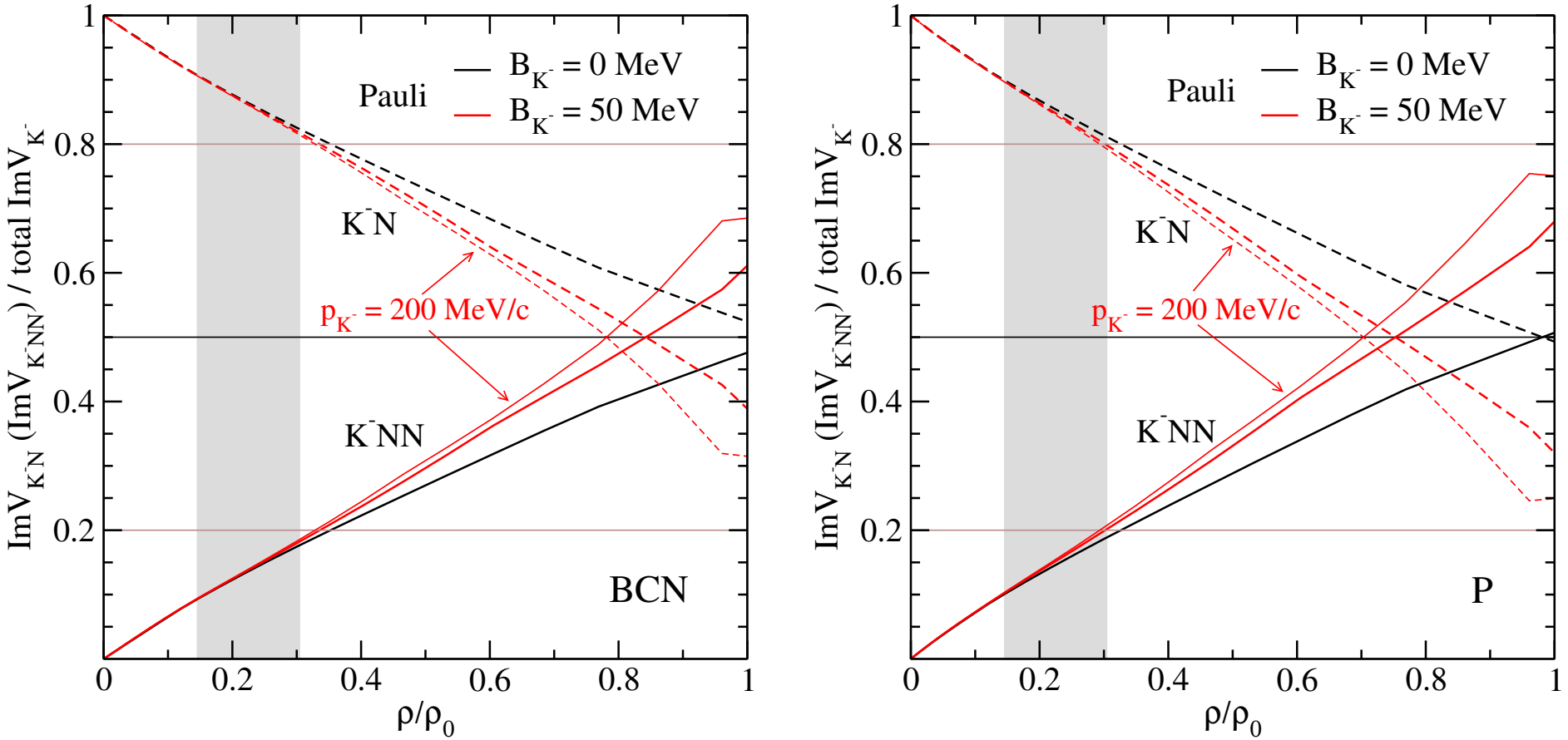

Fig.6: Ratio of K^- single-nucleon (K^-N) and two-nucleon (K^-NN) absorptive potentials to the total K^- absorptive potential as a function of relative density, calculated using the Pauli blocked amplitudes and for $B_{K-} = 0$ and 50 MeV and $p_{K-} = 0$ MeV/c and for $B_{K-} = 50$ MeV and $p_{K-} = 200$ MeV/c.

Cut-off dependence

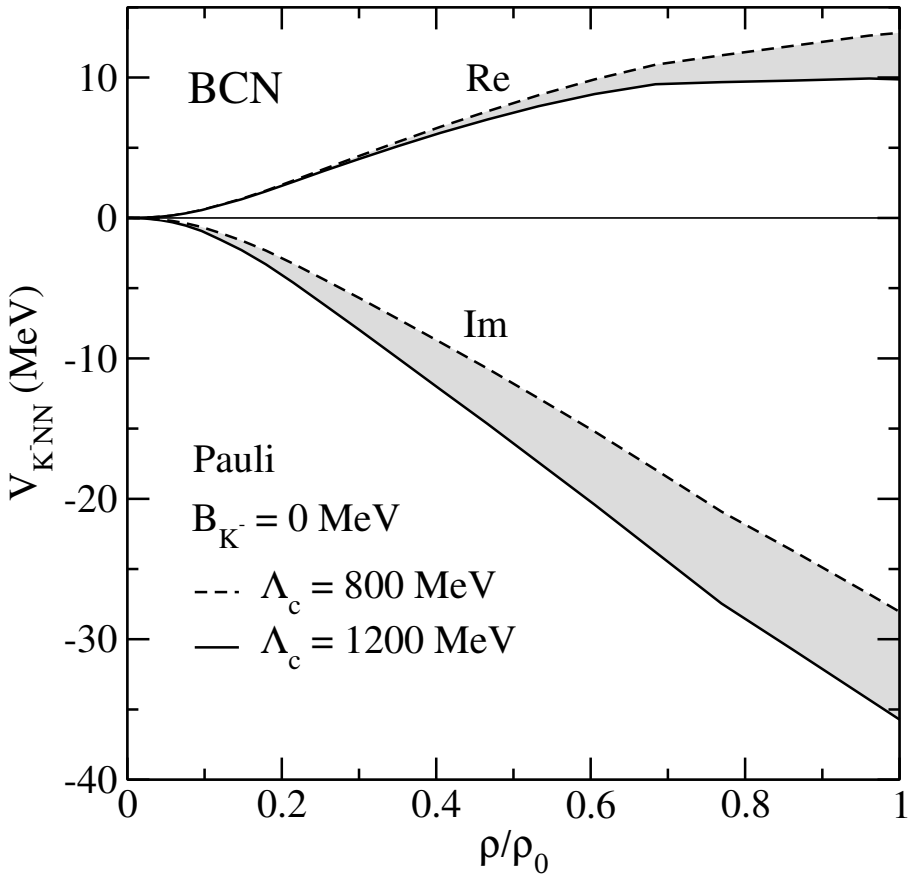

Fig.7: Dependence of the K^-NN potential on the value of the cut-off parameter Λ_c used in the form factors $F(\vec{q}) = \dfrac{\Lambda_C^2}{\Lambda_C^2 + \vec{q}^{\,2}}$, calculated for $B_{K^-} = 0$ MeV and $p_{K^-} = 0$ MeV/c with Pauli blocked BCN amplitudes.

AMADEUS data

- New measured ratio *R. Del Grande et al., EPJ C79 (2019) 190*

$$R = \frac{\mathrm{BR}(K^- pp \to \Lambda p)}{\mathrm{BR}(K^- pp \to \Sigma^0 p)} = 0.7 \pm 0.2(\mathrm{stat.})^{+0.2}_{-0.3}(\mathrm{syst.})$$

- Assumption that dominant contribution for $K^- pp \to \Lambda p$ and $K^- pp \to \Sigma^0 p$ channels comes from π^0 exchange leads to relation

$$\frac{\mathrm{BR}(K^- pp \to \Lambda p)}{\mathrm{BR}(K^- pp \to \Sigma^0 p)} = \frac{\mathrm{BR}(K^- p \to \pi^0 \Lambda)}{\mathrm{BR}(K^- p \to \pi^0 \Sigma^0)}$$

- However, the dominant contribution for $K^- pp \to \Lambda p$ channel comes from K^- exchange!

  T. Sekihara, D. Jido, Y. Kanada-En'yo, PRC 79 (2009) 062201(R)

  J. Hrtánková, À. Ramos, PRC 101 (2020) 035204

Ratio R for 2N absorption

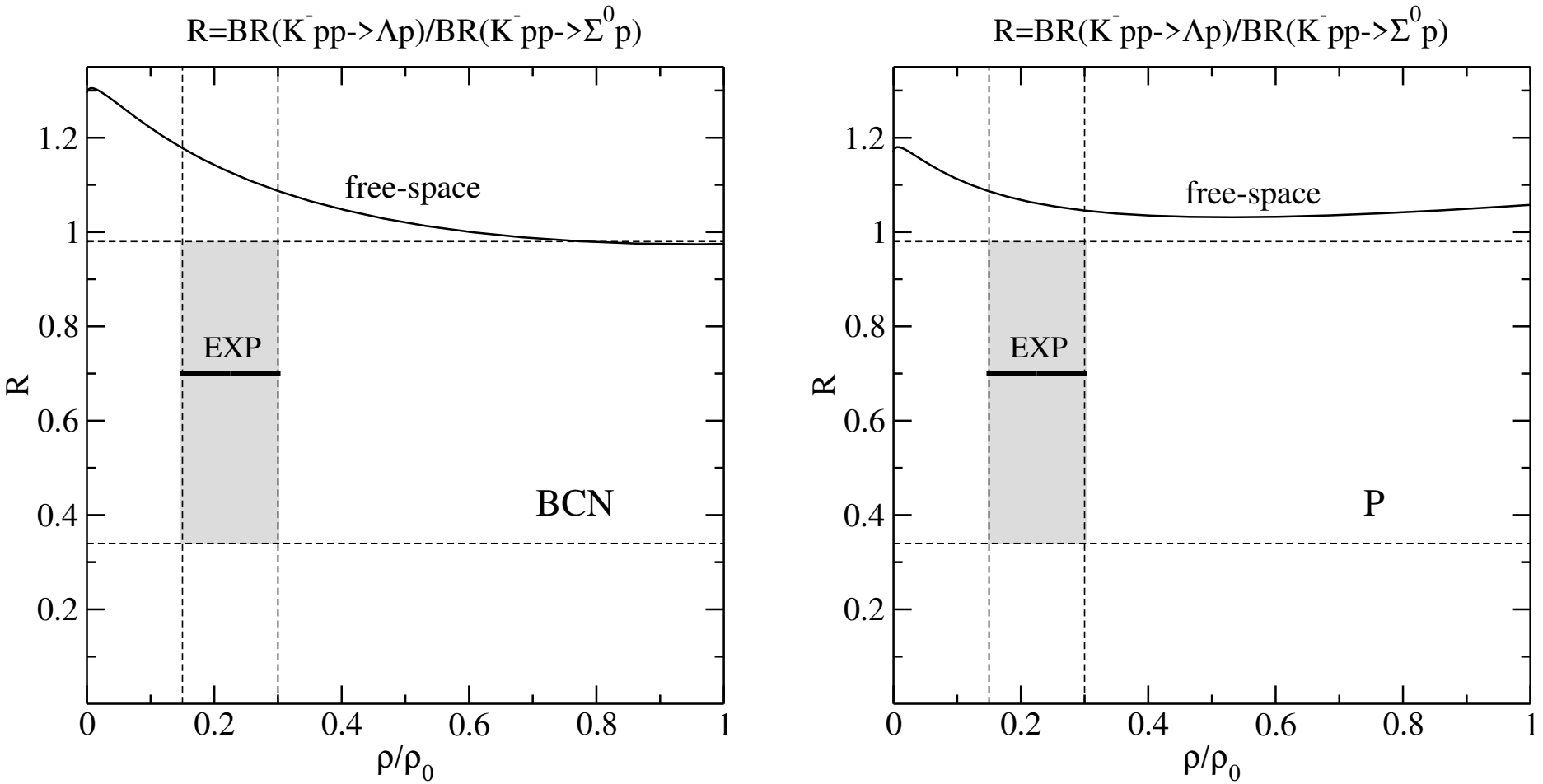

Fig.8: The ratio R as a function of relative density, calculated using the free-space amplitudes for $B_{K^-} = 0$ MeV. The dashed vertical lines denote the region of densities probed in experiments with low-energy K^- including the experimental value of the ratio with corresponding error bar.

Ratio R for 2N absorption

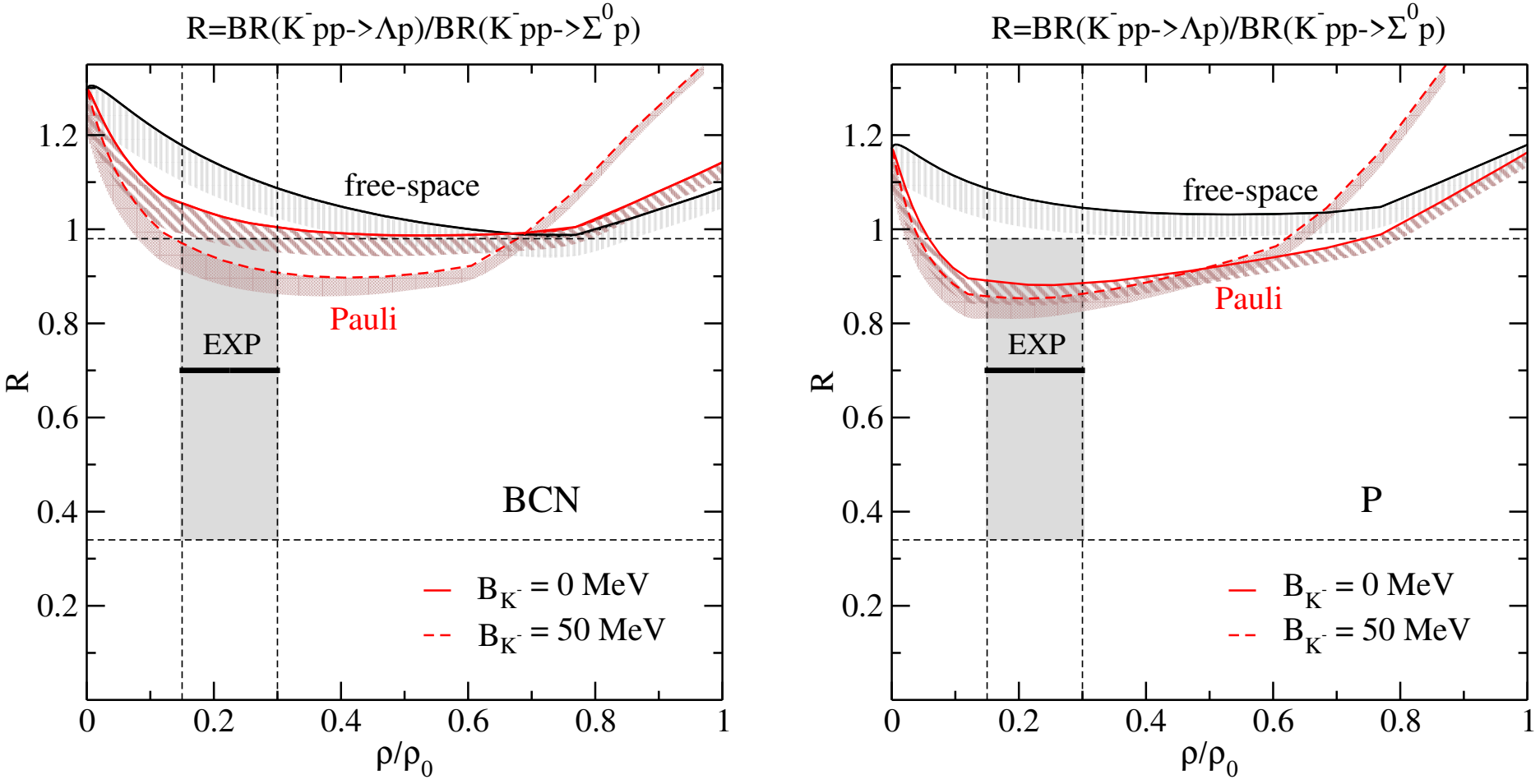

Fig.9: The ratio R as a function of relative density, calculated using the free-space and Pauli blocked amplitudes for $B_{K^-} = 0$ MeV and $B_{K^-} = 50$ MeV. Color bands denote the uncertainty due to different cut-off values $\Lambda_c = 800 - 1200$ MeV.

Ratio R^* for 1N absorption

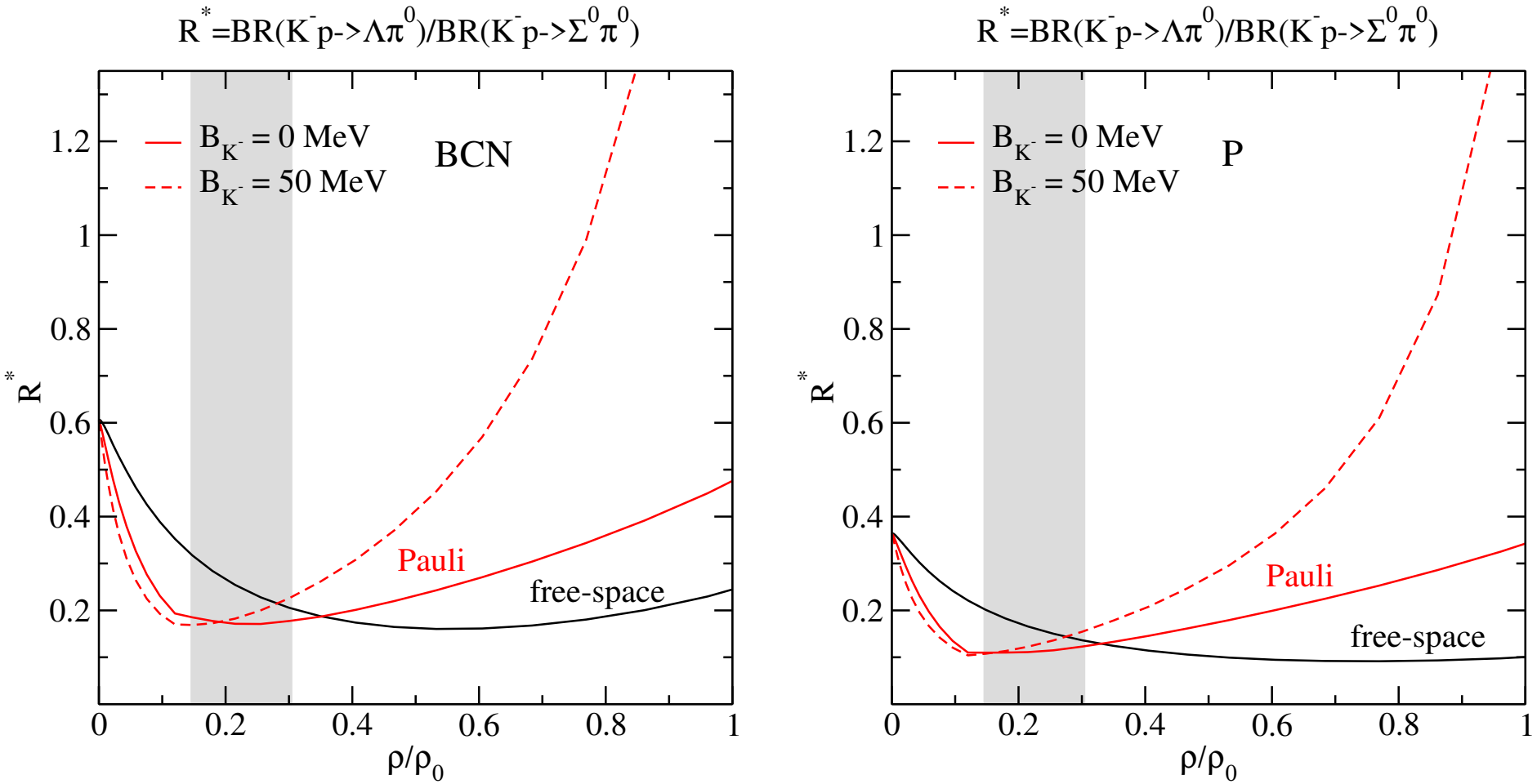

Fig.10: The ratio R^* as a function of relative density, calculated using the free-space and Pauli blocked amplitudes for $B_{K^-} = 0$ MeV and $B_{K^-} = 50$ MeV. The gray band denotes the region of densities probed in experiments with low-energy K^-.

Comparison with experimental data

Table 2: Primary-interaction ratios (in %) for mesonic absorption of K^- in nuclear matter, calculated with free-space and Pauli blocked BCN amplitudes for $B_{K^-} = 0$ MeV $p_{K^-} = 0$ MeV/c. The errors denote the uncertainty due to the cut-off dependence. The experimental data corrected for primary[a] interaction are shown for comparison.

BCN	$0.3\rho_0$		Exp. [1]	
mesonic ratio	f.s.	Pauli	^{4}He	^{12}C
$\Sigma^+\pi^-/K^-$	19.6 ± 0.6	28.8 ± 0.7	31.2 ± 5.0	29.4 ± 1.0
$\Sigma^-\pi^0/K^-$	6.2 ± 0.2	5.7 ± 0.1	4.9 ± 1.3	2.6 ± 0.6
$\Sigma^-\pi^+/K^-$	21.9 ± 0.6	14.8 ± 0.4	9.1 ± 1.6	13.1 ± 0.4
$\Sigma^0\pi^-/K^-$	6.2 ± 0.2	5.7 ± 0.1	4.9 ± 1.3	2.6 ± 0.6
$\Sigma^0\pi^0/K^-$	18.1 ± 0.5	19.2 ± 0.5	17.7 ± 2.9	20.0 ± 0.7
$\Lambda\pi^0/K^-$	3.8 ± 0.1	3.5 ± 0.1	5.2 ± 1.6	3.4 ± 0.2
$\Lambda\pi^-/K^-$	7.6 ± 0.2	7.0 ± 0.2	10.5 ± 3.0	6.8 ± 0.3
total 1N ratio	83.3 ± 2.4	84.6 ± 2.2	83.5 ± 7.1	77.9 ± 1.6

[a] Corrected for secondary interactions of the primary particles created in the absorbing nucleus.

[1] *C. Vander Velde-Wilquet et al., Nuovo Cimento 39 A (1977) 538*

Comparison with experimental data

Table 3: Primary-interaction total ratios (in %) for non-mesonic and total (1N+2N) K^- absorption in matter and corresponding ratios corrected for Σ-Λ conversion with different conversion rates, a) - 60% for Σ^+-Λ, 22.5% for Σ^--Λ, 72% for Σ^0-Λ, b) - 50% for all Σ's, calculated with Pauli blocked BCN amplitudes for $B_{K^-} = 0$ MeV. The errors denote the uncertainty due to the cut-off dependence.

BCN	$0.3\rho_0$	$0.3\rho_0$ + Σ-Λ conv.		Exp. [1]
non-mesonic ratio		a)	b)	^{4}He
$(\Lambda N + \Sigma^0 N)/K^-$	7.2 ± 1.1	10.5 ± 1.5	11.3 ± 1.6	11.7 ± 2.4
$(\Sigma^- N)/K^-$	4.3 ± 0.6	3.4 ± 0.4	2.2 ± 0.3	3.6 ± 0.9
$\Sigma^+ n/K^-$	3.8 ± 0.5	1.5 ± 0.2	1.9 ± 0.3	1.0 ± 0.4
$(\Sigma^0 N)/K^-$	3.7 ± 0.5	1.0 ± 0.1	1.9 ± 0.2	2.3 ± 1.0
total 2N ratio	15.4 ± 2.2	15.4 ± 2.2		16.4 ± 2.6
total ratio				
Σ^+/K^-	32.6 ± 0.2	13.0 ± 0.1	16.3 ± 0.1	17.0 ± 2.7
Σ^-/K^-	24.8 ± 0.1	19.21 ± 0.04	12.39 ± 0.03	13.8 ± 1.8
Σ^0/K^-	28.7 ± 0.1	8.03 ± 0.04	14.3 ± 0.1	10.8 ± 5.0
Λ/K^-	14.0 ± 0.3	59.7 ± 0.1	57.0 ± 0.2	58.4 ± 5.7
Σ^+/Σ^-	1.31 ± 0.01	0.68 ± 0.01	1.31 ± 0.01	1.2 ± 0.2

[1] *P. A. Katz et al., PRD 1 (1970) 1267*

Application to kaonic atoms

- K^-NN model applied in calculations of shifts and widths in kaonic atoms
- BCN amplitudes used $\rightarrow$ in-medium modifications included (Pauli or WRW) *T. Wass, M. Rho, W. Weise, NPA 617 (1997) 449*
- RMF densities and 2-parameter Fermi density distributions tested
- subthreshold kinematics taken from K^-NN model with $p_{K^-} = 150$ MeV/c

$$\sqrt{s} = \sqrt{(E_{K^-} + E_F)^2 - \tfrac{3}{5}k_F^2 - p_{K^-}^2}$$

RMF vs. 2pF densities check

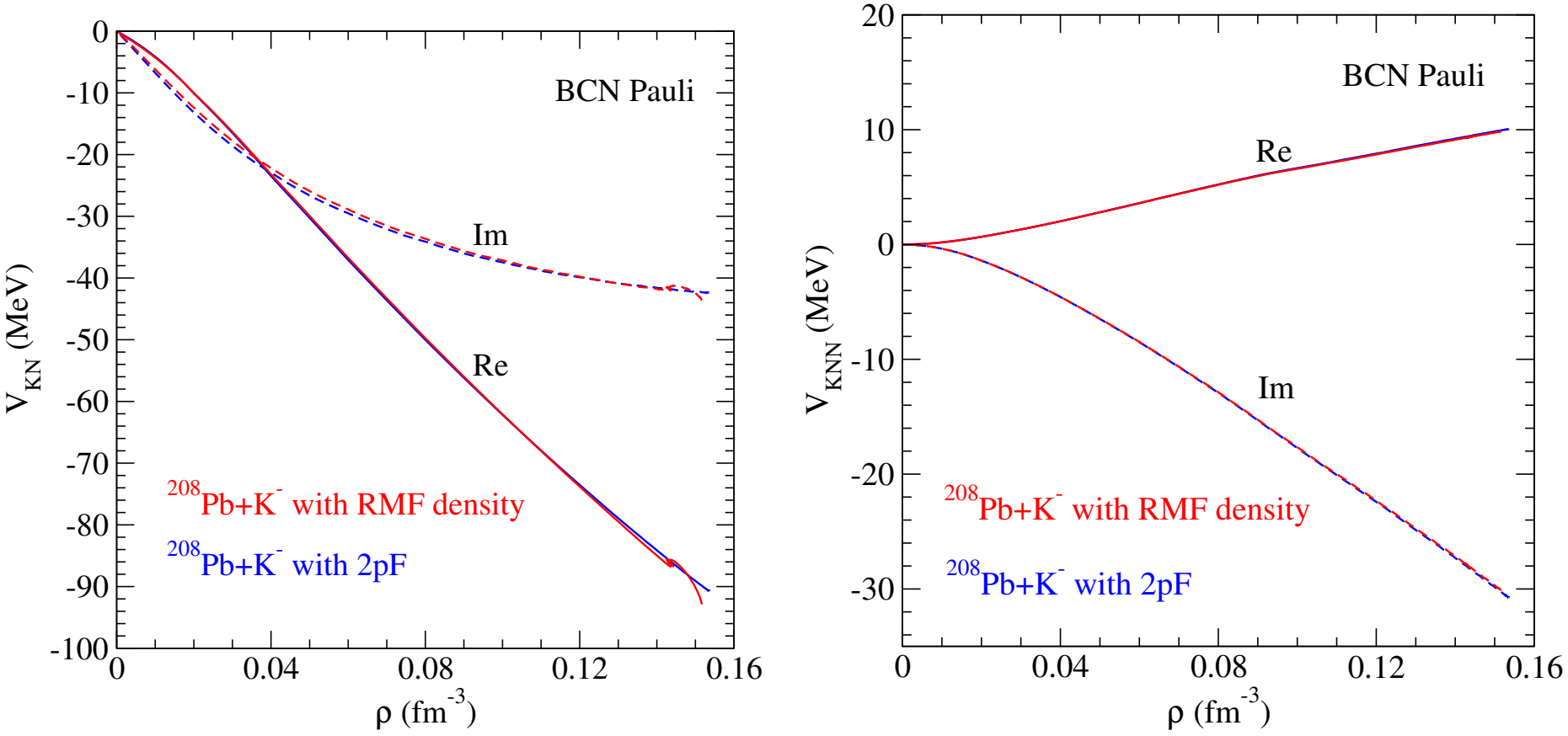

Fig.11: K^-N (left) and K^-NN (right) potentials in ^{208}Pb evaluated using RMF (red) and 2pF (blue) densities, calculated using Pauli BCN amplitudes.

Kaonic atoms calculations

Table 4: Values of χ^2 for shifts, widths and yields in selected K^- atoms, calculated with K^-N, $K^-N + K^-NN$ and K^-N+phen. multiN potentials based on BCN Pauli or WRW modified amplitudes. Experimental data are shown for comparison.

BCN		WRW		Pauli		phen.	EXP
		KN	+KNN	KN	+KNN	KN + phen. multiN	
C^{12}	$\Delta(\epsilon)$	74.81	20.85	8.46	4.63	0.53	-0.59 (0.08)
	Γ	22.68	21.38	9.46	5.27	1.77	1.73 (0.15)
	Γ^*	1.29	1.17	0.06	0.57	2.45	0.99 (0.20)
P^{31}	$\Delta(\epsilon)$	23.23	6.14	1.84	1.82	0.07	-0.33 (0.08)
	Γ	10.49	12.96	6.02	4.63	0.78	1.44 (0.12)
	Γ^*	7.40	5.96	0.70	0.42	0.42	1.89 (0.30)
S^{32}	$\Delta(\epsilon)$	324.03	134.55	74.54	77.37	15.81	-0.494 (0.038)
	Γ	20.73	40.37	5.35	3.50	0.57	2.19 (0.10)
	Γ^*	37.82	31.30	20.62	14.05	6.47	3.03 (0.44)
Cl^{35}	$\Delta(\epsilon)$	18.81	7.4	0.80	1.15	0.00	-0.99 (0.17)
	Γ	0.26	6.08	3.60	2.70	0.27	2.91 (0.24)
	Γ^*	8.78	5.32	0.60	0.24	0.17	5.8 (1.70)
Cu^{63}	$\Delta(\epsilon)$	9.31	0.43	0.20	0.56	1.23	-0.370 (0.047)
	Γ	0.05	0.46	1.33	1.40	2.23	1.37 (0.17)
	Γ^*	1.39	0.16	0.25	0.47	1.44	5.2 (1.1)
Sn^{118}	$\Delta(\epsilon)$	2.52	2.57	4.71	5.12	3.23	-0.41 (0.18)
	Γ	0.06	0.06	0.06	0.25	0.45	3.18 (0.64)
	Γ^*	22.83	14.44	6.31	5.72	4.09	15.1 (4.4)
Pb^{208}	$\Delta(\epsilon)$	0.12	0.50	0.13	0.41	1.14	-0.02 (0.012)
	Γ	0.09	0.06	0.21	0.29	0.41	0.37 (0.15)
	Γ^*	0.11	0.26	0.39	0.44	0.50	4.1 (2)
χ^2	total	586.82	312.43	145.62	131.01	44.00	
	S^{32}out	204.24	106.20	45.10	36.09	21.16	

Kaonic atoms calculations

- best χ^2 obtained for K^-N + mic. K^-NN potentials evaluated using Pauli blocked BCN amplitudes and $p_{K^-} = 150$ MeV/c (other values of p_{K^-} were considered as well)
- these $K^-N + K^-NN$ potentials were calculated for 23 targets and confronted with kaonic atom data $\rightarrow \chi^2(65)$=338.2 (5.20 per point)
- $K^-N + K^-NN$ potentials then supplemented by phenomenological term describing 3 and 4 nucleon processes $\sim -4\pi B(\frac{\rho}{\rho_0})^\alpha \rho$
- values of α and complex amplitude B fitted to data

Fit to kaonic atom data #1: Re$B > 0$

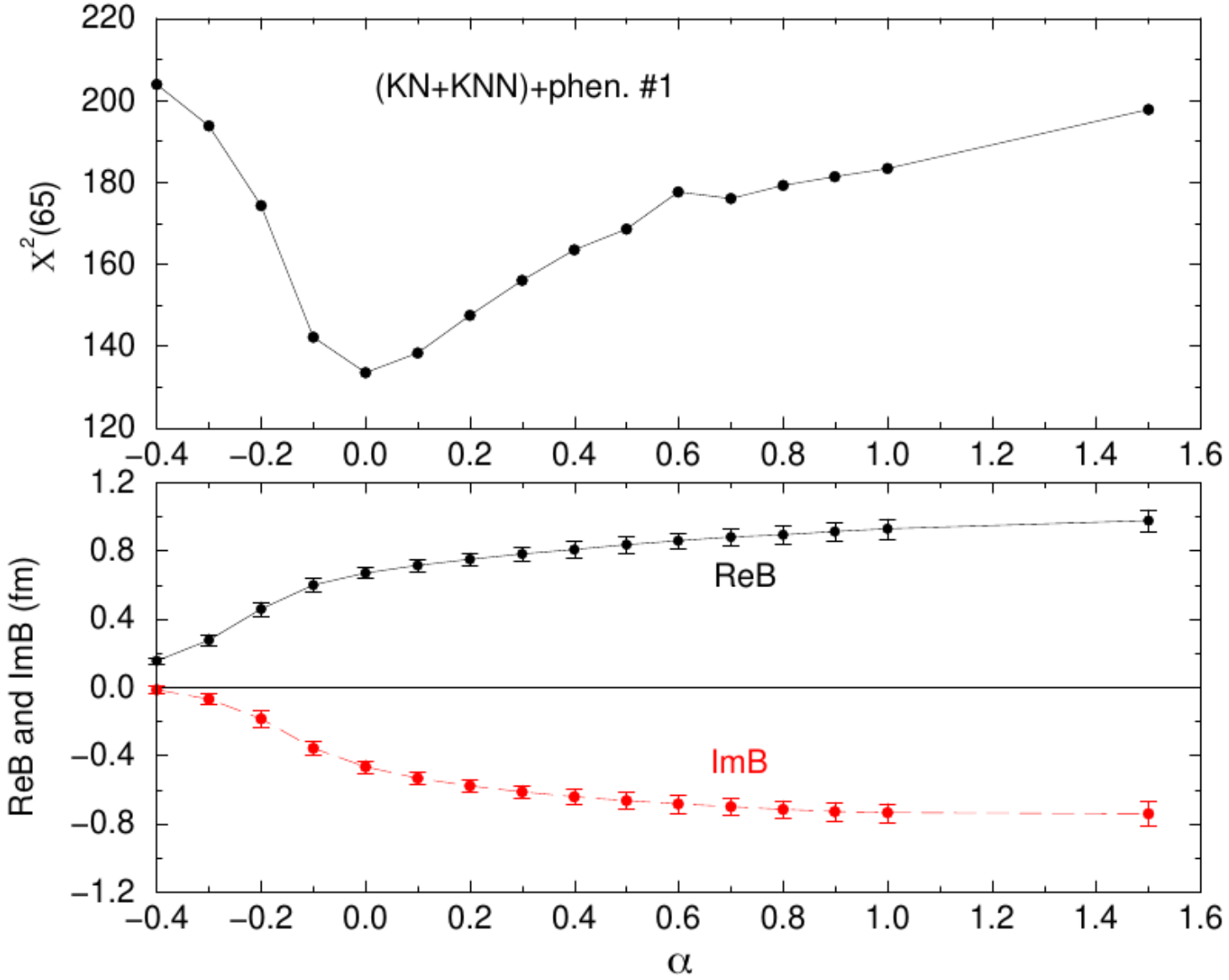

Fit to kaonic atom data #2: Re$B < 0$

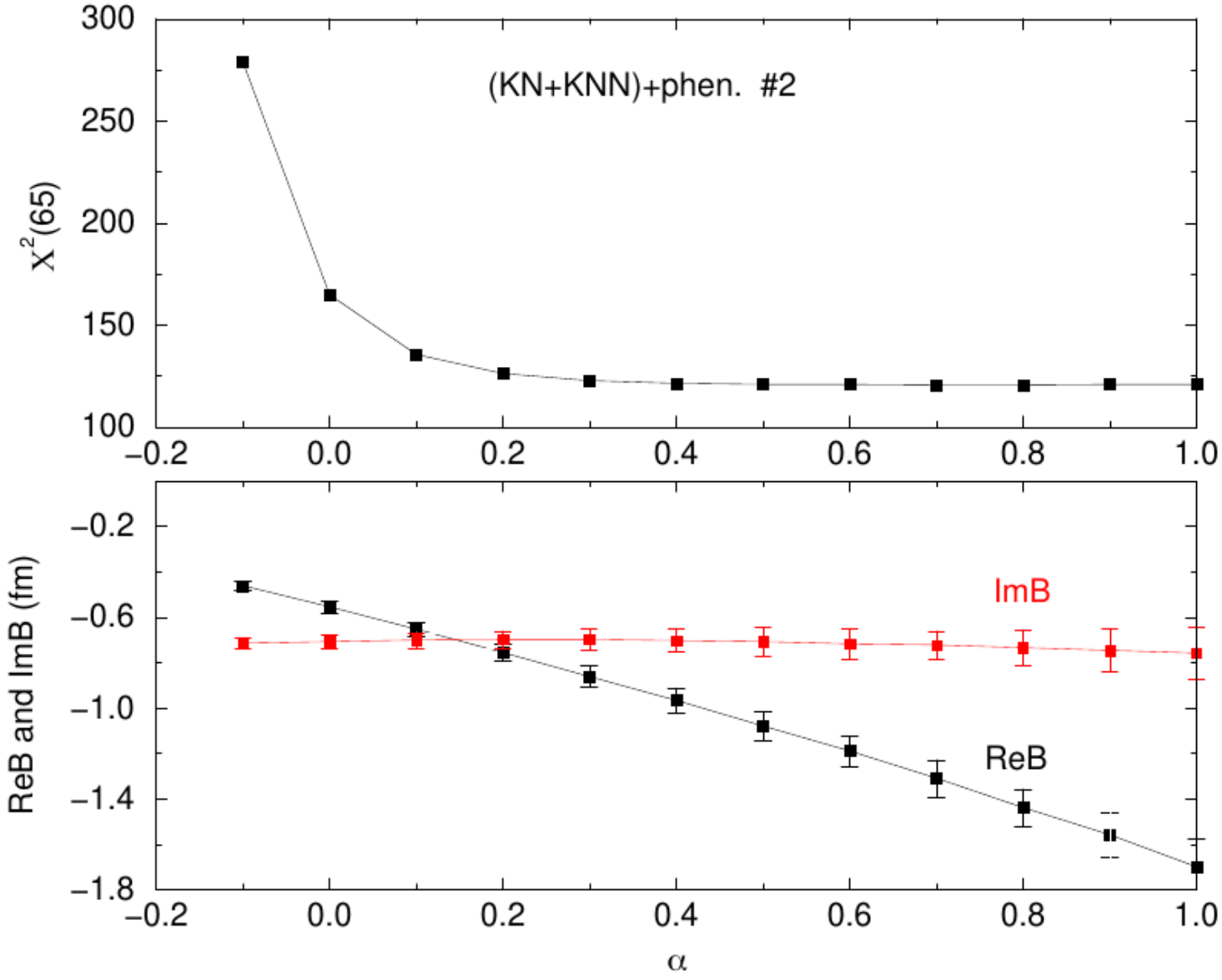

Results

- #1 $\alpha = 0.00 \pm 0.04$, Re$B = 0.66 \pm 0.04$ fm, Im$B = -0.46 \pm 0.04$ fm
- #2 $\alpha > 0.3$, ReB and Im$B < 0$
- $K^-N \to K^-N + K^-NN \to K^-N + K^-NN$+phen.term

	K^-N	$K^-N + K^-NN$	+ phen.	K^-N+phen.
$\chi^2(65)$	2829	338.2	133	112.3
χ^2/d.p.	43.8	5.2	2.1	1.7

- additional fit with rescaled potential $\beta_{SF}(K^-N + K^-NN) \to$ Re$\beta_{SF} = 1.68 \pm 0.027$ and Im$\beta_{SF} = 0.57 \pm 0.022$ and $\chi^2(65) = 113$

Results

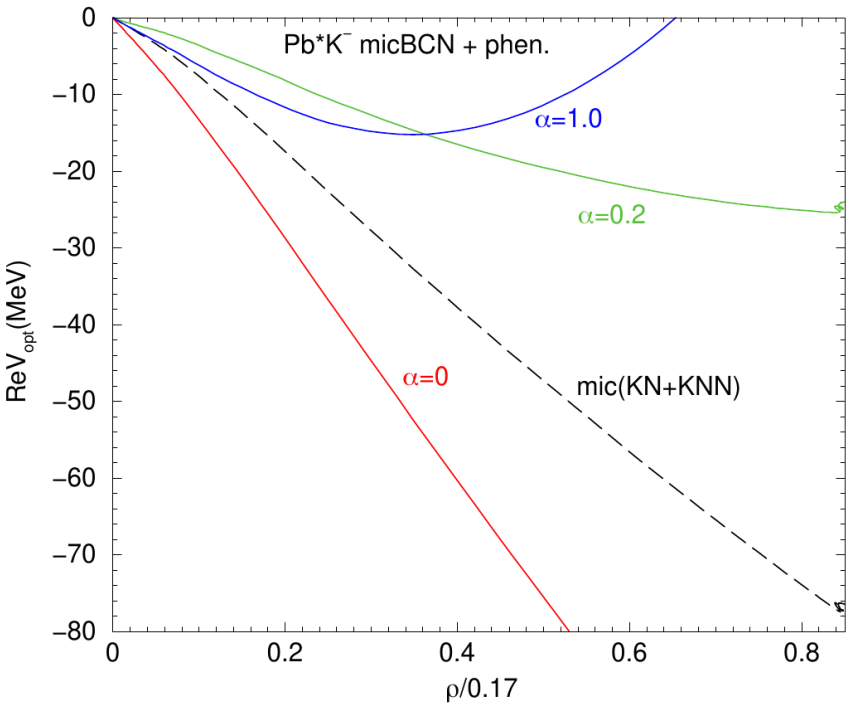
Pb*K⁻ micBCN + phen.
α=1.0
α=0.2
α=0
mic(KN+KNN)
ReV_opt(MeV)
ρ/0.17
0
−10
−20
−30
−40
−50
−60
−70
−80
0
0.2
0.4
0.6
0.8

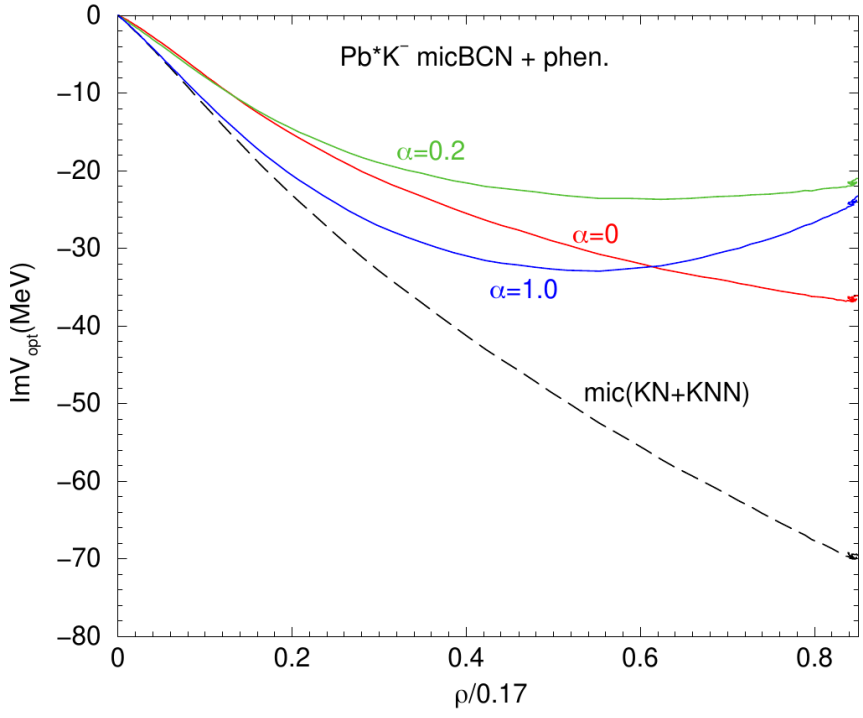
Pb*K⁻ micBCN + phen.
α=0.2
α=0
α=1.0
mic(KN+KNN)
ImV_opt(MeV)
ρ/0.17
0
−10
−20
−30
−40
−50
−60
−70
−80
0
0.2
0.4
0.6
0.8

Conclusions: K^-NN model

- Interaction of K^- with two and more nucleons important for realistic description of K^--nucleus interaction
- We have developed a microscopic model for K^-NN absorption in nuclear matter using scattering amplitudes derived from P and BCN chiral meson-baryon interaction models

  J. Hrtánková, À. Ramos, PRC 101 (2020) 035204
- Pauli blocked amplitudes included $\rightarrow$ medium effects non-negligible
- Calculated ratios in a good agreement with experimental data!

Conclusions: kaonic atoms calculations

- The microscopic K^-NN model was applied in the calculations of kaonic atoms
- Preliminary results:
  - data are best described by $K^-N + K^-NN$ potentials based on Pauli blocked BCN amplitudes
  - $K^-N + K^-NN$ potentials supplemented by a phenomenological term describing 3 and 4 nucleon processes
  - fit to the data suggests that $\mathrm{Re}(K^-N + K^-NN)$ should be more attractive and $\mathrm{Im}(K^-N + K^-NN)$ should be less absorptive

What to do next?

- test more values for $p_{K^-}(= 0, 100$ MeV/c, LDA...)
- different approach to $\sqrt{s}$ from studies of kaonic atoms
- confront with data $K^-N + K^-NN$ potentials based on WRW modified amplitudes
- include missing baryon self-energies in in-medium modified amplitudes
- self-consistent approach